

Fig. 4. Attenuation versus shutter position.

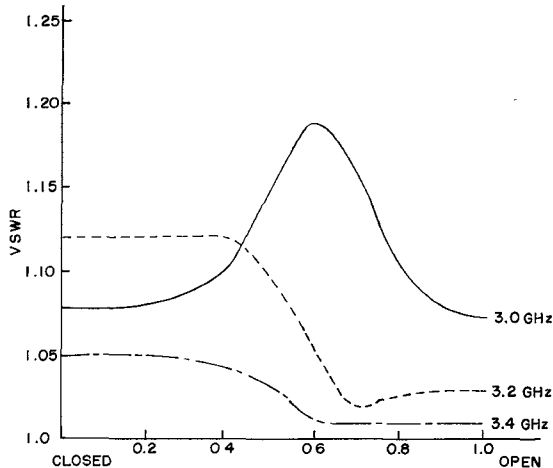


Fig. 5. VSWR versus shutter position.

The power divider has operated satisfactorily at power levels of up to 700 kW and has exhibited a dynamic range of power division in excess of 36 dB. When the RF shutters were adjusted throughout their full range of movement, operating at 200 kW peak, no visible shift in the transmitter frequency was observed.

VSWR and attenuation measurements were conducted at frequencies from 2.8 to 3.6 GHz at a 70 mW power level. The results from 3.0 to 3.4 GHz are shown in Figs. 4 and 5.

For maximum power division the power divider should be operated within the passband of the coupler. The attenuation was 34.2 dB at 3.1 GHz and 36.7 dB at 3.2 GHz, while outside the passband the maximum attenuation was only 25 dB at 3.6 GHz and 18 dB at 2.8 GHz. The VSWR remained below 1.20 over the test band. The VSWR of the loads did not exceed 1.09.

At a peak power level of 500 kW, it was

possible to vary the power output from a high value of 500 kW peak to a minimum of 160 watts peak. This is an actual high-power dynamic range of 35 dB.

Colloidal graphite powder is used to eliminate binding of the RF shutter. After 100 to 200 hours of operation, the power divider is taken apart and cleaned and lubricated. For more positive control of the power adjustment, future models will employ a rack-and-pinion or worm-gear drive. The size and weight of the device can be substantially reduced by employing commercially available adapter fittings and loads.

The basic concept for the microwave power divider described was conceived jointly by the author and F. Jellison of Microwave Associates, Inc., Burlington, Mass.

ROBERT M. TRUE  
Electronic Components Lab.  
USAECOM  
Fort Monmouth, N. J.

## Controlled Wideband Differential Phase Shifters Using Varactor Diodes

For phased array transmitting systems diode step phase shifters of limited bandwidth have been developed. Thereby PIN diodes are used because they switch high peak power with low loss. In certain receiving systems and in most microwave measurements, however, a continuous phase adjustment is required. Thus, low power analog phase shifters covering broad frequency bands are desirable. This correspondence describes an electronically-controlled three-port network using varactor diodes, which produces a constant phase difference between the two output ports.

This three-port consists of a power divider at the input and two coaxial lines, each loaded by identical series reactances at equal spacings (Fig. 1). In one of these lines the reactances are inductive, while in the other they are capacitive such that the phase versus frequency responses have equal gradients in the prescribed frequency band (Fig. 2). Thus the phase difference will be independent of frequency. The reactances are realized with varactor diodes controlled by reverse bias. The equivalent circuit of the diode mounted in series with the inner conductor of the coaxial line consists basically of an inductance in series with the diode junction capacitance. This arrangement provides positive reactance if the series resonance of the diode is below, and negative reactance if the diode resonance is above the operating frequency.

In the equivalent circuit representation at the diode in its holder, the transition from the coaxial line center conductor to the crystal is approximated by a stepped geometry [Fig. 3(a)]. Each constant diameter section ( $T_0-T_1$ ,  $T_1-T_2$ , etc.) is considered as a short piece of homogeneous transmission line which is sufficiently short to be represented by an equivalent series inductance and two shunt capacitances. Furthermore the stray fields excited by each diameter step are taken into account by additional shunt capacitances. The spring and crystal are represented by a lead inductance  $L_s$ , a series resistance  $R_s$ , and the junction capacity  $C_j$ . Capacitances between the facing surfaces  $T_0-T_0'$ ,  $T_1-T_1'$ , and  $T_2-T_2'$  must also be considered. Numerical values of the equivalent circuit elements are such that the circuit can be simplified considerably. Thus, all shunt capacitances can be lumped into single shunt capacitances at the reference planes  $T_0$  and  $T_0'$  as shown in Fig. 3(b). In the actual networks, the values of  $L_s$  and  $C_j$  have been measured by a method similar to that given by Roberts,<sup>1</sup> whereas  $R_s$  has been determined by Crook's method.<sup>2</sup> The remaining reactances, which depend on the dimensions of the line, have been evaluated by approximation formulas<sup>3</sup> and verified experimentally.

Manuscript received March 6, 1967; revised June 1, 1967.

<sup>1</sup> D. Roberts, "Measurements of varactor diode impedance," *Trans. Microwave Theory and Techn'ques*, vol. MTT-12, pp. 471-475, July 1964.

<sup>2</sup> D. Crook, "A simplified technique for measuring high quality varactor parameters," *Solid State Design*, vol. 6, pp. 31-33, August 1965.

<sup>3</sup> C. Liechti, "Steuerbare, breitbandige Differenzphasenschieber mit Kapazitätsdioden im Mikrowellengebiet," Dissertation No. 3926, Swiss Federal Institute of Technology, Zurich, Switzerland, 1967.

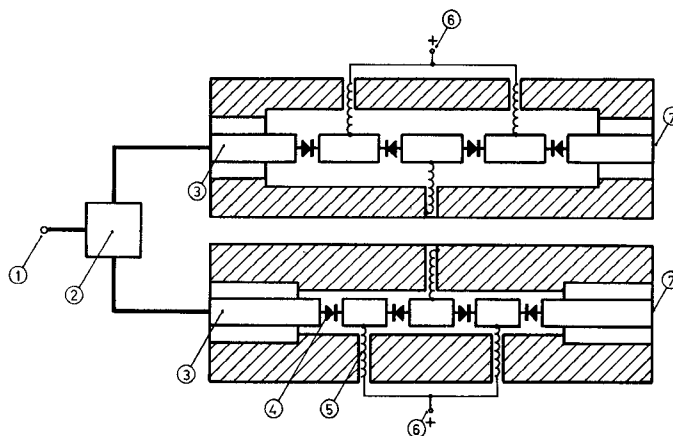


Fig. 1. Differential phase shifter: 1) input, 2) power divider, 3) coaxial transmission lines, 4) varactor diode, 5) helical line, 6) control voltage, and 7) output ports.

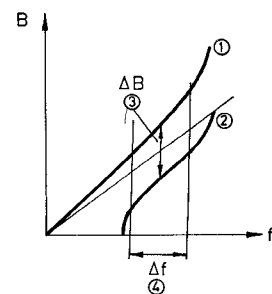


Fig. 2. Phase response of the periodically loaded transmission lines: 1) phase of the inductively loaded line, 2) phase of the capacitively loaded line, 3) phase difference of the two networks, and 4) operating frequency range.

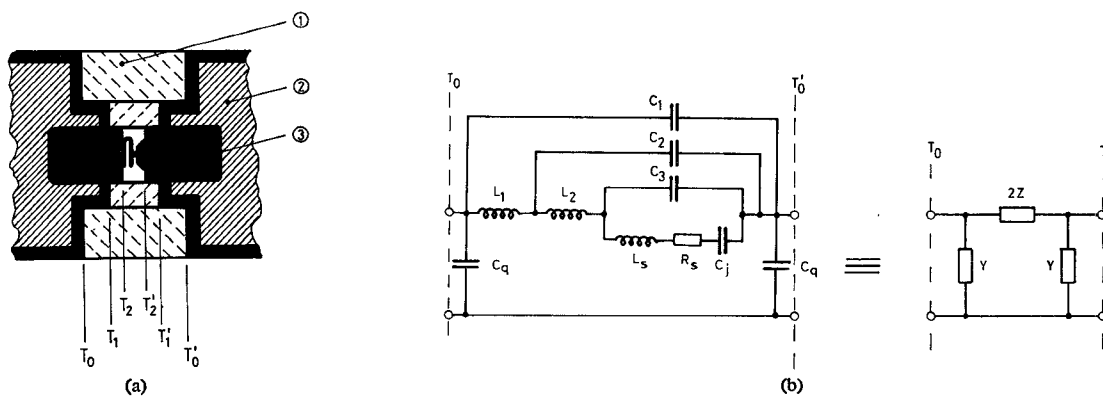


Fig. 3. (a) The packaged diode mounted in the center conductor of the coaxial line: 1) additional dielectric sleeve, 2) center conductor, and 3) diode. (b) The equivalent circuit.

The two phase controlling networks contain  $n$  cascaded identical basic sections, each consisting of a varactor diode between two coaxial lines of length  $l/2$  and characteristic impedance  $Z_0$ . The transformation matrix of this two port is given by

$$\begin{bmatrix} a_{11} & a_{12} \\ a_{21} & a_{22} \end{bmatrix} = \begin{bmatrix} \cos \frac{\beta l}{2} & j \sin \frac{\beta l}{2} \\ j \sin \frac{\beta l}{2} & \cos \frac{\beta l}{2} \end{bmatrix} \cdot \begin{bmatrix} 1 + 2yz & 2z \\ 2y(1 + yz) & 1 + 2yz \end{bmatrix} \cdot \begin{bmatrix} \cos \frac{\beta l}{2} & j \sin \frac{\beta l}{2} \\ j \sin \frac{\beta l}{2} & \cos \frac{\beta l}{2} \end{bmatrix} \quad (1)$$

where  $\beta = 2\pi/\lambda$  and the small letters refer to the impedances, normalized with respect to  $Z_0$ . The impedances can be decomposed into real and imaginary parts ( $z = r + jx$  and  $y = jb$ ). It is observed that  $r \ll 1$  holds for most practical cases. Hence, the image transfer constant  $K = A + jB$  is given by the following expressions:

$$\cosh K = a_{11} \quad (2)$$

$$B \approx \arccos \{ (1 - 2bx) \cos (\beta l) - [b + x(1 - b^2)] \sin (\beta l) \} \quad (3)$$

$$A \approx r \frac{2b \cos (\beta l) + (1 - b^2) \sin (\beta l)}{\sin B} \quad (4)$$

The image impedance  $Z_0'$  is expressed by

$$Z_0' = \frac{a_{12}}{\sinh K} \quad (5)$$

and

$$Z_0' \approx \frac{[x(1 - b^2) + b] \cos (\beta l) + [1 - 2bx] \sin (\beta l) + x(1 + b^2) - b}{\sin B} \quad (6)$$

From these equations the transmission and reflection characteristics of the  $n$  sections, terminated on both ports with the characteristic impedance of the adjacent transmission line, can be determined.

For the synthesis of a network with given specifications the number of diodes, hence, an equivalent number of basic sections connected in cascade, is determined by the desired maximum phase deviation. The diode spacing is chosen for optimum linearity of phase response. The characteristic impedance of the coaxial sections between the diodes is selected to match the terminating transmis-

sion lines for a mean series reactance. The tuning range necessary for the junction capacity  $C_j$  is determined by the prescribed range of differential phase. Furthermore a proper choice of the inductances  $L_1 + L_2$  and the capacitance  $C_3$  [Fig. 3(b)] results in equal slopes of the two phase responses at midband

frequency, and for two distinct values of  $C_j$ . Finally, the allowable insertion loss determines the maximum value of the series resistance  $R_s$ .

For an experimental verification of theory and design approach, a two phase network has been designed with a differential phase shift variable between 0 and 90 degrees for a frequency range from 2.8 to 4.2 GHz. Four varactor diodes have been incorporated in each of the two coaxial lines for which theoretical and measured results are shown in Fig. 4. The curves agree sufficiently to justify the network calculation on the basis of the diode

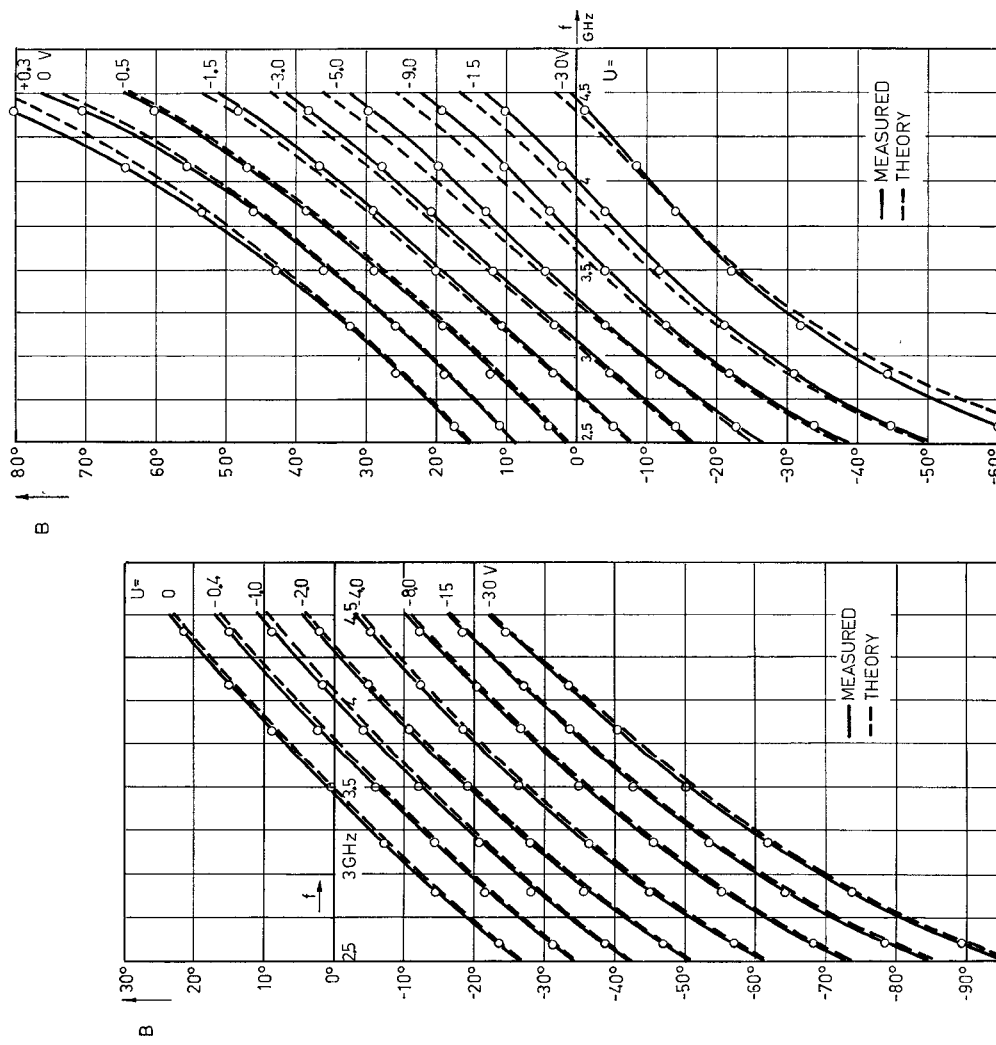


Fig. 4. (a) Phase response of the capacitively loaded line with the diode bias voltage as parameter. (b) Phase response of the inductively loaded line with the diode bias voltage as parameter.

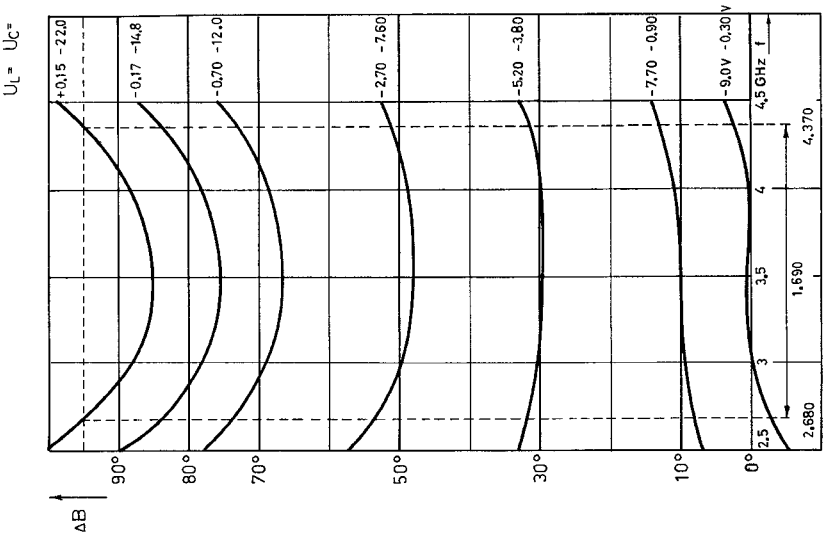


Fig. 5. Phase difference  $\Delta B$  between the two networks as a function of frequency.  $U_L$  is the bias voltage applied to the diodes of the inductively loaded line,  $U_C$  is the bias voltage applied to the diodes of the capacitively loaded line, and  $\Delta f$  is the frequency range such that the phase difference deviates less than  $\pm 5$  degrees from the nominal value.

equivalent circuit. The phase difference of suitably paired response curves is given in Fig. 5, the phase error is seen to be below  $\pm 5$  degrees in this experimental arrangement. At higher power levels additional phase errors may occur due to increase of the effective junction capacitance in a nonlinear capacitor. Further errors result from rectification and resulting change of bias and from heating of the junction.

Diodes having a cutoff frequency of 40 GHz (at -6 volts) were used in the experimental circuit. Attenuation is a function of phase<sup>3</sup> and with these diodes the maximum and minimum values of the attenuation differed by less than 1.8 dB over the whole phase and frequency range which agreed well with the theoretical expectations. However, for better diodes with a breakdown voltage of -24 volts and cutoff frequency of 160 GHz (at -6 volts) this difference in attenuation would be only 0.5 dB, which is acceptable for most applications.

The reflection factor at the input of the phase shifter was less than 20 percent. If better matching is required, substantially smaller reflection factors can be achieved by using end half sections.

Finally, it should be mentioned that feeding the bias voltage to the center conductor through helical lines proved to be very successful. The helical lines were made long enough to provide enough attenuation at the signal frequency, so that they appear to be terminated by their characteristic impedance. The main transmission line with a characteristic impedance of approximately 50 ohms is loaded only imperceptibly by the high impedance of the helical lines (2.3 k $\Omega$ ). The rise-time of the bias voltage in this arrangement was less than 30 ns.

C. A. LIECHTI  
G. W. EPPRECHT  
Microwave Lab.  
Swiss Federal Inst. of Tech.  
Zürich, Switzerland

## Bandwidth Curves for Mumford's Maximally Flat Filter

In 1963, Mumford published design tables for a maximally flat symmetrical bandpass filter composed of six or fewer shorted quarterwave stubs separated by quarterwave lines of unit impedance.<sup>1</sup> The tables were extended to ten stubs in 1965.<sup>2</sup> These tables list the stub normalized admittances  $k_i$  for given values of  $n$  (the number of stubs) and a bandwidth-related parameter ( $10 \log K_n$ ) calculated from the  $k_i$ .

The bandwidth curves given here (Fig. 1) are supplementary design information which were computed from Mumford's formula for insertion loss

$$\frac{P_0}{P_L} = 1 + K_n \frac{(\cos \theta)^{2n}}{(\sin \theta)^2} \quad (1)$$

where  $\theta = 2\pi L/\lambda$ ,  $L$  is the length of a stub, and  $\lambda$  is the wavelength at center frequency in the passband. The curves serve a twofold purpose. First, they give the relative 3 dB bandwidth  $w$  as a function of ( $10 \log K_n$ ) and  $n$ . Here,

$$w = (f_2 - f_1)/f_0 = 2(f_0 - f_s)/f_0 \quad (2)$$

where  $(f_2 - f_1)$  is the 3 dB bandwidth and  $f_0$  is the center frequency. Second, they permit the determination of attenuation  $L_s$  at frequency  $f_s$  for values of attenuation  $L_s > 15$  dB. Thus, at the two edges of the band centered at  $f_0$

$$w_s = |2(f_0 - f_s)/f_0| \quad (3)$$

we have

$$L_s \approx 10 \log_{10} K_n - (10 \log_{10} K_n)_s \quad (4)$$

Manuscript received April 27, 1967.

<sup>1</sup> W. W. Mumford, "An exact design technique for a type of maximally flat quarter-wave coupled band pass filter," *IEEE-PGMMT Nat'l Symp. Prog. and Digest*, pp. 57-61, May 1963.

<sup>2</sup> W. W. Mumford, "Tables of stub admittances for maximally flat filters using shorted quarter-wave stubs," *IEEE Trans. Microwave Theory and Techniques (Correspondence)*, vol. MTT-13, pp. 695-696, September 1965.

where the first term on the right side is the same as previously described, and the second term (with subscript  $s$ ) is obtained from the bandwidth curves of Fig. 1 for any chosen (high-attenuation) bandwidth  $w_s > w$ .

The following example will explain the use of the bandwidth curves. Consider the design of a six-stub filter with a specified 3 dB bandwidth  $w = 0.72$ . (This value was chosen to allow comparison with the trial-design insertion-loss curve in Fig. 1 of Mumford,<sup>1</sup> which has the same relative 3 dB bandwidth.) First, enter Fig. 1 at  $w = 0.72$  on the ( $n=6$ ) curve. We obtain  $10 \log K_6 = 30.5$  which may then be used to find, by interpolation in Mumford's table, the normalized admittances  $k_i$  for a six-stub filter. (This calculation will be left to the interested reader.) Next, assuming the center frequency of the filter to be 900 MHz, as in Mumford's example, find the attenuation at 425 MHz. First, using (3), calculate  $w_s = 2(900 - 425)/900 = 1.06$ . Entering Fig. 1 again, we obtain  $(10 \log K_n)_s = 12.5$ , then by (4),  $L_s = 30.5 - 12.5 = 18$  dB, which checks closely with Mumford's Fig. 1.<sup>1</sup>

For values of attenuation near zero frequency (or near the center of the upper stopband), the attenuation  $L_s$  depends mainly on the value of  $K_n$  and the frequency, and is relatively independent of the number of stubs  $n$ . This is seen in Fig. 1 for large values of bandwidth approaching the upper limit  $w_s = 2$ . The reason for this characteristic of  $L_s$  is the well-known fact that, regardless of the value of  $n$ , there is only one pole of attenuation at zero frequency for the shorted quarterwave stub configuration of a bandpass filter. A useful formula for computing the attenuation near zero frequency is

$$L_s(w_s \rightarrow 2) \approx 10 \log K_n - 20 \log \left(1 - \frac{w_s}{2}\right) - 4 \text{ dB.} \quad (5)$$

B. M. SCHIFFMAN  
Stanford Research Inst.  
Stanford, Calif.

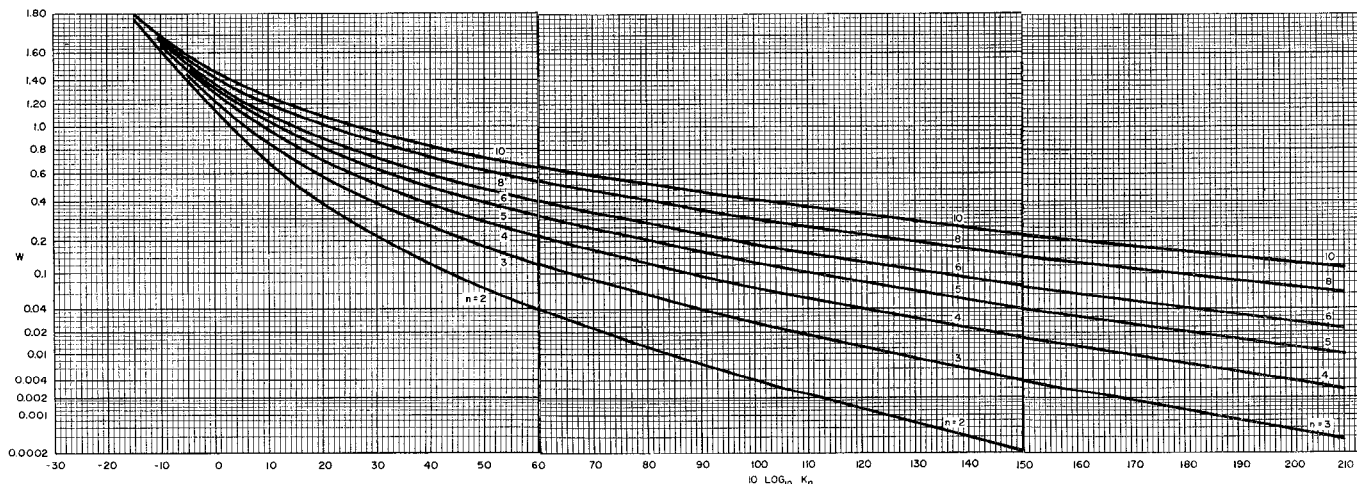


Fig. 1. Relative bandwidth  $w$  plotted against filter design parameter ( $10 \log_{10} K_n$ ) for Mumford's maximally flat filter.